

To Smooth or Not to Smooth?

Bias and Efficiency in fMRI Time-Series Analysis

K. J. Friston,* O. Josephs,* E. Zarahn,† A. P. Holmes,* S. Rouquette,‡ and J.-B. Poline‡

*The Wellcome Department of Cognitive Neurology, Institute of Neurology, Queen Square, London WC1N 3BG, United Kingdom;

†Department of Neurology, University of Pennsylvania, Philadelphia, Pennsylvania 19104; and

‡CEA/DSV/DRM/SHFJ, 4 Place General Leclerc, 91406 Orsay, France

Received July 28, 1999

This paper concerns temporal filtering in fMRI time-series analysis. Whitening serially correlated data is the most efficient approach to parameter estimation. However, if there is a discrepancy between the assumed and the actual correlations, whitening can render the analysis exquisitely sensitive to bias when estimating the standard error of the ensuing parameter estimates. This bias, although not expressed in terms of the estimated responses, has profound effects on any statistic used for inference. The special constraints of fMRI analysis ensure that there will always be a misspecification of the assumed serial correlations. One resolution of this problem is to filter the data to minimize bias, while maintaining a reasonable degree of efficiency. In this paper we present expressions for efficiency (of parameter estimation) and bias (in estimating standard error) in terms of assumed and actual correlation structures in the context of the general linear model. We show that: (i) Whitening strategies can result in profound bias and are therefore probably precluded in parametric fMRI data analyses. (ii) Band-pass filtering, and implicitly smoothing, has an important role in protecting against inferential bias. © 2000 Academic Press

Key Words: functional neuroimaging; fMRI; bias; efficiency; filtering; convolution; inference.

INTRODUCTION

This paper is about serial correlations in fMRI time series and their impact upon the estimations of, and inferences about, evoked hemodynamic responses. In Friston *et al.* (1994), we introduced the statistical complications that arise, in the context of the general linear model (or linear time invariant systems), due to temporal autocorrelations or “smoothness” in fMRI time series. Since that time a number of approaches to these intrinsic serial correlations have been proposed and our own approach has changed substantially over the years. In this paper we describe briefly the sources

of correlations in fMRI error terms and consider different ways of dealing with them. In particular we consider the importance of filtering the data to condition the correlation structure despite the fact that removing correlations (i.e., whitening) would be more efficient. These issues are becoming increasingly important with the advent of event-related fMRI that typically evokes responses in the higher frequency range (Paradis *et al.*, 1998).

This paper is divided into three sections. The first describes the nature of, and background to, serial correlations in fMRI and the strategies that have been adopted to accommodate them. The second section comments briefly on the implications for optimum experimental design and the third section deals, in greater depth, with temporal filtering strategies and their impact on efficiency and robustness. In this section we deal first with efficiency and bias for a single serially correlated time series and then consider the implications of spatially varying serial correlations over voxels.

SERIAL CORRELATIONS IN fMRI

fMRI time series can be viewed as a linear admixture of signal and noise. Signal corresponds to neuronally mediated hemodynamic changes that can be modeled as a linear (Friston *et al.*, 1994) or nonlinear (Friston *et al.*, 1998) convolution of some underlying neuronal process, responding to changes in experimental factors. fMRI noise has many components that render it rather complicated in relation to other neurophysiological measurements. These include neuronal and nonneuronal sources. Neuronal noise refers to neurogenic signal not modeled by the explanatory variables and occupies the same part of the frequency spectrum as the hemodynamic signal itself. These noise components may be unrelated to the experimental design or reflect variations about evoked responses that are inadequately modeled in the design matrix. Nonneuronal components can have a physiological (e.g., Meyer’s waves) or

nonphysiological origin and comprise both white [e.g., thermal (Johnston) noise] and colored components [e.g., pulsatile motion of the brain caused by cardiac cycles or local modulation of the static magnetic field (B_0) by respiratory movement]. These effects are typically low frequency (Holmes *et al.*, 1997) or wide band (e.g., aliased cardiac-locked pulsatile motion). The superposition of these colored components creates serial correlations among the error terms in the statistical model (denoted by \mathbf{V}_i below) that can have a severe effect on sensitivity when trying to detect experimental effects. Sensitivity depends upon (i) the relative amounts of signal and noise and (ii) the efficiency of the experimental design and analysis. Sensitivity also depends on the choice of the estimator (e.g., linear least squares vs Gauss–Markov) as well as the validity of the assumptions regarding the distribution of the errors (e.g., the Gauss–Markov estimator is the maximum likelihood estimator only if the errors are multivariate Gaussian as assumed in this paper).

There are three important considerations that arise from this signal processing perspective on fMRI time series: The first pertains to optimum experimental design, the second to optimum filtering of the time series to obtain the most efficient parameter estimates, and the third to the robustness of the statistical inferences about the parameter estimates that ensue. In what follows we will show that the conditions for both high efficiency and robustness imply a variance–bias trade-off that can be controlled by temporal filtering. The particular variance and bias considered in this paper pertain to the variance of the parameter estimates and the bias *in estimators of this variance*.

The Background to Serial Correlations

Serial correlations were considered initially from the point of view of statistical inference. It was suggested that instead of using the number of scans as the degrees of freedom for any statistical analysis, the effective degrees of freedom should be used (Friston *et al.*, 1994). The effective degrees of freedom were based upon some estimate of the serial correlations and entered into the statistic so that its distribution under the null hypothesis conformed more closely to that expected under parametric assumptions. The primary concern at this stage was the *validity* of the inferences that obtained. This heuristic approach was subsequently corrected and refined, culminating in the framework described in Worsley and Friston (1995). In Worsley and Friston (1995) a general linear model was described that accommodated serial correlations, in terms of both parameter estimation and inference using the associated statistics. In order to avoid estimating the intrinsic serial correlations, the data were convolved with a Gaussian smoothing kernel to impose an approximately known correlation structure. The criti-

cal consideration at this stage was *robustness* in the face of errors in estimating the correlations. Bullmore *et al.* (1996) then proposed an alternative approach, whereby the estimated temporal autocorrelation structure was used to prewhiten the data, prior to fitting a general linear model with assumed identical and independently distributed error terms. This proposal was motivated by considerations of *efficiency*. Validity and robustness were ensured in the special case of the analysis proposed by Bullmore *et al.* (1996) because they used randomization strategies for inference.¹ Variations on an autoregressive characterization of serial correlations then appeared. For example Locascio *et al.* (1997) used autoregressive moving average (ARMA) models on a voxel-by-voxel basis. Purdon and Weisskoff (1998) suggested the use of an AR(1) plus white noise model. In the past years a number of empirical characterizations of the noise have been described. Among the more compelling is a modified $1/f$ characterization² of Aguirre *et al.* (1997) and Zarahn *et al.* (1997) (see Appendix A for a more formal description of autoregressive and modified $1/f$ models). In short, there have emerged a number of apparently disparate approaches to dealing with, and modeling, noise in fMRI time series. Which of these approaches or models is best? The answer to this question can be framed in terms of efficiency and robustness.

Validity, Efficiency, and Robustness

Validity refers to the validity of the statistical inference or the accuracy of the P values that are obtained from an analysis. A test is valid if the false-positive rate is less than the nominal specificity (usually $\alpha = 0.05$). An exact test has a false-positive rate that is equal to the specificity. The efficiency of a test relates to the estimation of the parameters of the statistical model employed. This estimation is more efficient when the variability of the estimated parameters is smaller. A test that remains valid for a given departure from an assumption is said to be robust to violation of that assumption. If a test becomes invalid, when the assumptions no longer hold, then it is not a robust test. In general, considerations of efficiency are subordinate to ensuring that the test is valid under the normal circumstances of its use. If these circumstances incur some deviation from the assumptions behind the test, robustness becomes the primary concern.

¹ There is an argument that the permutation of scans implicit in the randomization procedure is invalid if serial correlations persist after whitening: Strictly speaking the scans are not interchangeable. The strategy adopted by Bullmore *et al.* (1996) further assumes the same error variance for every voxel. This greatly reduces computational load but is not an assumption that everyone accepts in fMRI.

² This class of model should not be confused with conventional $1/f$ processes with fractal scaling properties, which are $1/f$ in power. The models referred to as “modified $1/f$ models” in this paper are $1/f$ in amplitude.

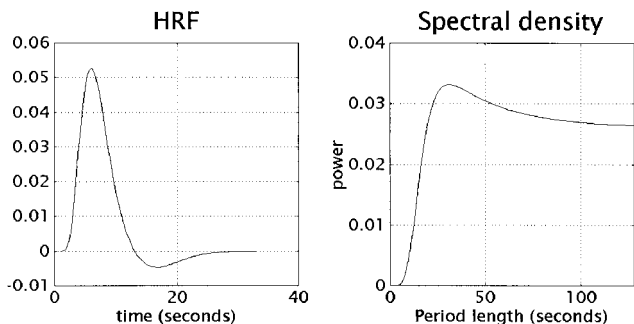


FIG. 1. Left: A canonical hemodynamic response function (HRF). The HRF in this instance comprises the sum of two gamma functions modeling a peak at 6 s and a subsequent undershoot. Right: Spectral density associated with the HRF expressed as a function of 1/frequency or period length. This spectral density is $|l(\omega)|^2$ where $l(\omega)$ is the HRF transfer function.

OPTIMUM EXPERIMENTAL DESIGN

Any linear time invariant model (e.g., Friston *et al.*, 1994; Boynton *et al.*, 1996) of neurally mediated signals in fMRI suggests that only those experimental effects whose frequency structure survives convolution with the hemodynamic response function (HRF) can be estimated with any efficiency. Experimental variance should therefore be elicited with reference to the transfer function of the HRF. The corresponding frequency profile of a canonical transfer function is shown in Fig. 1 (right). It is clear that frequencies around 1/32 Hz will be preserved, following convolution, relative to other frequencies. This frequency characterizes periodic designs with 32-s periods (i.e., 16-s epochs). Generally the first objective of experimental design is to comply with the natural constraints imposed by the HRF and to ensure that experimental variance occupies these intermediate frequencies.

Clearly there are other important constraints. An important one here is the frequency structure of noise, which is much more prevalent at low frequencies (e.g., 1/64 Hz and lower). This suggests that the experimental frequencies, which one can control by experimental design, should avoid these low-frequency ranges. Other constraints are purely experimental; for example, psychological constraints motivate the use of event-related designs that evoke higher frequency signals (Paradis *et al.*, 1998) relative to equivalent block designs. Typical regressors for an epoch- or block-related design and an event-related design are shown in Fig. 2. The epoch-related design is shown at the top and comprises a box-car and its temporal derivative, convolved with a canonical HRF (shown on the left in Fig. 1). An event-related design, with the same number of trials presented in a stochastic fashion, is shown at the bottom. Again the regressors correspond to an underlying set of delta functions (“stick” function) and their temporal derivatives convolved with a canonical HRF. The

event-related design has more high-frequency components and this renders it less efficient than the block design from a statistical perspective (but more useful from other perspectives). The regressors in Fig. 1 will be used later to illustrate the role of temporal filtering.

TEMPORAL FILTERING

This section deals with temporal filtering and its effect on efficiency and inferential bias. We start with the general linear model and derive expressions for efficiency and bias in terms of assumed and actual correlations and some applied filter. The next subsection shows that the most efficient filtering scheme (a *minimum variance filter*) introduces profound bias into the estimates of standard error used to construct the test statistic. This results in tests that are insensitive

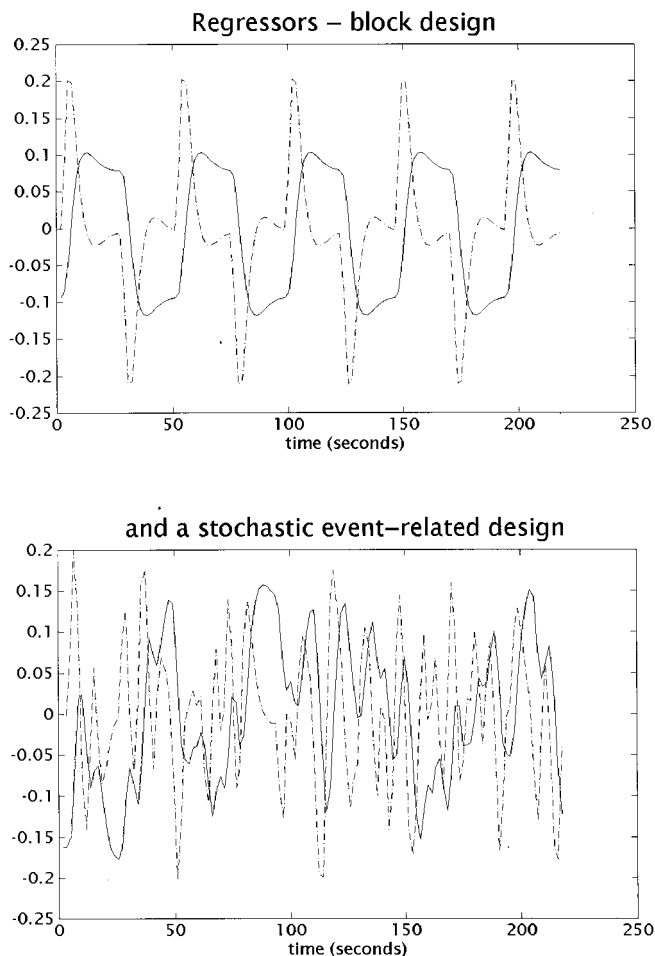


FIG. 2. Regressors for an epoch-related or block design (top) and an event-related design (bottom) with 128 scans and a TR of 1.7 s. Both sets of regressors were constructed by convolving the appropriate stimulus function (box-car for the block design and a stick function for the event-related design) and its temporal derivative with the canonical HRF depicted in Fig. 1. These regressors have been orthogonalized and Euclidean normalized.

or potentially invalid (i.e., not robust). The position adopted in this paper is that, for fMRI data analysis, a minimum variance filter is not appropriate. Instead we would like to find a *minimum bias filter*. This is difficult because one needs to know how the serial correlations that are likely to be encountered deviate from the assumed form. The next subsection presents a way of estimating the expected bias and efficiency, given the probability distribution of the intrinsic correlations. Using empirical estimates of this distribution it is shown that suppressing both high and low frequencies with band-pass filtering is required to minimize bias. The expected values for bias and efficiency are then used to compare three filtering strategies, (i) whitening, (ii) high-pass, and (iii) band-pass (i.e., high pass with smoothing) filtering, under different models of the correlations. In brief it will be shown that supplementing high-pass filtering with smoothing has an important role in reducing bias whatever model is assumed. This section concludes by noting that minimizing bias over a range of deviations from the assumed form for the correlations also renders bias less sensitive to spatial variations in serial correlations from voxel to voxel.

Efficiency and Bias

Here we provide expressions for the efficiency and bias for any experimental design, embodied in the explanatory variables or regressors that comprise the design matrix \mathbf{X} and any contrast or compound of parameter estimates specified with a vector of contrast weights. Consider the general linear model

$$\mathbf{S}\mathbf{y} = \mathbf{S}\mathbf{X}\boldsymbol{\beta} + \mathbf{S}\mathbf{K}_i\mathbf{z}, \quad (1)$$

where \mathbf{y} is a $(n \times 1)$ response variable (measured fMRI signal at any voxel) and \mathbf{S} is an extrinsic or applied temporal filter matrix. If \mathbf{S} has a Toeplitz form then it can be considered as an applied (de)convolution. However, generally \mathbf{S} can take any form. A distinction is made between the true intrinsic correlations and those assumed. These correlations are characterized by the $(n \times n)$ convolution matrices \mathbf{K}_i and \mathbf{K}_a , respectively, with an ensuing noise process $\mathbf{K}_i\mathbf{z}$ where \mathbf{z} is an independent innovation $\sim \mathcal{N}(0, \sigma^2\mathbf{I})$.

The corresponding autocorrelation matrices are $\mathbf{V}_i = \mathbf{K}_i\mathbf{K}_i^T$ and $\mathbf{V}_a = \mathbf{K}_a\mathbf{K}_a^T$. The general least-squares estimator of the parameters is

$$\hat{\boldsymbol{\beta}}_{\text{GLS}} = (\mathbf{X}^T\mathbf{S}^T\mathbf{S}\mathbf{X})^{-1}(\mathbf{S}\mathbf{X})^T\mathbf{S}\mathbf{y} = (\mathbf{S}\mathbf{X})^+\mathbf{S}\mathbf{y}, \quad (2)$$

where $^+$ denotes the pseudoinverse. The efficiency of estimating a particular contrast of parameters is inversely proportional to the contrast variance,

$$\text{var}\{\mathbf{c}^T\hat{\boldsymbol{\beta}}_{\text{GLS}}\} = \sigma^2\mathbf{c}^T(\mathbf{S}\mathbf{X})^+\mathbf{S}\mathbf{V}_i\mathbf{S}^T(\mathbf{S}\mathbf{X})^+\mathbf{c}, \quad (3)$$

where \mathbf{c} is a vector of contrast weights. One might simply proceed by choosing \mathbf{S} to maximize efficiency or, equivalently, minimize contrast variance (see “Minimum Variance Filters”). However, there is another important consideration here: any statistic used to make an inference about the significance of the contrast is a function of that contrast and an *estimate* of its variance. This second estimate depends upon an estimate of σ^2 and an estimate of the intrinsic correlations \mathbf{V}_i (i.e., \mathbf{V}_a). The estimator of the contrast variance will be subject to bias if there is a mismatch between the assumed and the actual correlations. Such bias would invalidate the use of theoretical distributions, of test statistics derived from the contrast, used to control false-positive rates.

Bias can be expressed in terms of the proportional difference between the true contrast variance and the expectation of its estimator (see Appendix B for details),

$$\begin{aligned} \text{Bias}\{\mathbf{S}, \mathbf{V}_i\} \\ = 1 - \frac{\text{trace}\{\mathbf{R}\mathbf{S}\mathbf{V}_i\mathbf{S}^T\}\mathbf{c}^T(\mathbf{S}\mathbf{X})^+\mathbf{S}\mathbf{V}_a\mathbf{S}^T(\mathbf{S}\mathbf{X})^+\mathbf{c}}{\text{trace}\{\mathbf{R}\mathbf{S}\mathbf{V}_a\mathbf{S}^T\}\mathbf{c}^T(\mathbf{S}\mathbf{X})^+\mathbf{S}\mathbf{V}_i\mathbf{S}^T(\mathbf{S}\mathbf{X})^+\mathbf{c}}, \end{aligned} \quad (4)$$

where $\mathbf{R} = \mathbf{I} - \mathbf{S}\mathbf{X}(\mathbf{S}\mathbf{X})^+$ is a residual-forming matrix. When bias is less than zero the estimated standard error is too small and the ensuing T or F statistic will be too large, leading to capricious inferences (i.e., false positives). When bias is greater than zero the inference will be too conservative (but still valid). In short if $\mathbf{K}_i \neq \mathbf{K}_a$ then bias will depend on \mathbf{S} . If $\mathbf{K}_i = \mathbf{K}_a$ then bias = 0 but efficiency still depends upon \mathbf{S} .

Minimum Variance Filters

Conventional signal processing approaches and estimation theory dictate that whitening the data engenders the most efficient parameter estimation. This corresponds to filtering with a convolution matrix \mathbf{S} that is the inverse of the intrinsic convolution matrix \mathbf{K}_i (where $\mathbf{K}_i = \mathbf{V}_i^{1/2}$). The resulting parameter estimates are optimally efficient among all linear, unbiased estimators and correspond to the maximum likelihood estimators under Gaussian assumptions. More formally, the general least-squares estimators $\hat{\boldsymbol{\beta}}_{\text{GLS}}$ are then equivalent to the Gauss–Markov or linear minimum variance estimators $\hat{\boldsymbol{\beta}}_{\text{GM}}$ (Lawson and Hanson, 1974).

In order to whiten the data one needs to know, or estimate, the intrinsic correlation structure. This reduces to finding an appropriate model for the autocorrelation function or spectral density of the error terms and then estimating the parameters of that model. Clearly one can never know the true structure but we can compare different models to characterize their relative strengths and weaknesses. In this paper we will take a high-order (16) autoregressive model as the

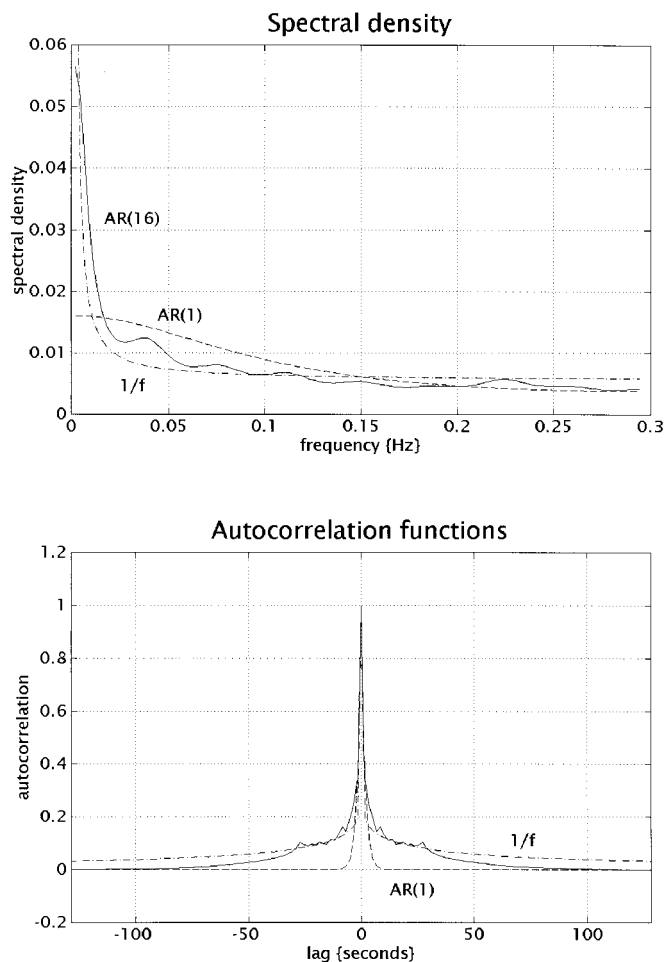


FIG. 3. Spectral densities (top) and corresponding autocorrelation functions (bottom) for the residual terms of a fMRI time series averaged over 512 voxels. Three cases are shown: (i) An AR(16) model estimated using the Yule–Walker method (this is taken to be a good approximation to the true correlations). The “bump” in the spectrum at around 1/32 Hz may reflect harmonics of random variations in trial-to-trial responses (every 16 s). (ii) An AR(1) model estimate using the same method. (iii) For a model of the form $(q_1/f + q_2)$ where f is frequency in Hz. These data came from a single-subject, event-related, single-word-presentation fMRI study acquired with multislice EPI at 2 T with a TR of 1.7 s. The words were presented every 16 s. The data were globally normalized, and fitted event-related responses (Josephs *et al.*, 1997) were removed. The 512 voxels were selected on the basis of a nontrivial response to acoustic stimulation, based on the F ratio in a conventional SPM analysis ($P < 0.001$ uncorrected). This ensured that the ensuing gray-matter voxels represented a fairly homogeneous population in terms of their functional specialization.

“gold standard” and evaluate simpler, but commonly used, models in relation to it. In other words we will consider the AR(16) model as an approximation to the true underlying correlations. The problem of estimating serial correlations is highlighted in Fig. 3. Here the residuals from a long (512-scan, TR = 1.7 s) time series were used to estimate the spectral density and associated autocorrelation functions (where one is the

Fourier transform of the other) using the Yule–Walker method with an autoregression order of 16 (see Appendix A). The data came from a single-subject event-related study using sparse single-word presentations every 16 s. Evoked responses were removed following global normalization. Estimates of the autocorrelation functions and spectral densities using a commonly assumed AR(1) model (Bullmore *et al.*, 1996) and a modified $1/f$ model (Zarahn *et al.*, 1997) are also shown. The AR(1) is inadequate in that it fails to model either long-range (i.e., low frequencies) or intermediate correlations. The modified $1/f$ model shown here is a good approximation for the short-range and intermediate correlations but fails to model the long-range correlations as well as it could. Any discrepancy between the assumed and the actual correlation structure means that, when the data are whitened in accord with the assumed models, the standard error of the contrast is biased. This leads directly to bias in the ensuing statistics. For example the T statistic is simply the quotient of the contrast and its estimated standard error. It should be noted that the simple models would fit much better if drifts were first removed from the time series. However, this drift removal corresponds to high-pass filtering and we want to make the point that filtering is essential for reducing the discrepancy between assumed and actual correlations (see below).

This bias is illustrated in Fig. 4 under a variety of model-specific minimum-variance filters. Here the regressors from the epoch- and event-related designs in Fig. 2 were used as the design matrix \mathbf{X} , to calculate the contrast variance and bias in the estimate of this variance according to Eq. (3) and Eq. (4), where

$$\mathbf{V}_i = \mathbf{V}_{\text{AR}(16)},$$

$$\mathbf{V}_a = \begin{Bmatrix} \mathbf{V}_i \\ \mathbf{V}_{\text{AR}(1)} \\ \mathbf{V}_{1/f} \\ \mathbf{1} \end{Bmatrix}, \quad \mathbf{S} = \begin{Bmatrix} \mathbf{K}_i^{-1} & \text{“correct” model} \\ \mathbf{K}_{\text{AR}(1)}^{-1} & \text{AR(1) model} \\ \mathbf{K}_{1/f}^{-1} & 1/f \text{ model} \\ \mathbf{1} & \text{“none”} \end{Bmatrix}.$$

The variances in Fig. 4 have been normalized by the minimum variance possible (i.e., that of the “correct” model). The biases are expressed in terms of the proportion of variance incorrectly estimated. Obviously the AR(16) model gives maximum efficiency and no bias (bias = 0) because we have used the AR(16) estimates as an approximation to the actual correlations. Any deviation from this “correct” form reduces efficiency and inflates the contrast variance. Note that misspecifying the form for the serial correlations has inflated the contrast variance more for the event-related design (bottom) relative to the epoch-related design (top). This is because the regressors in the epoch-related design correspond more closely to eigenvectors of the intrinsic autocorrelation matrix (see Worsley

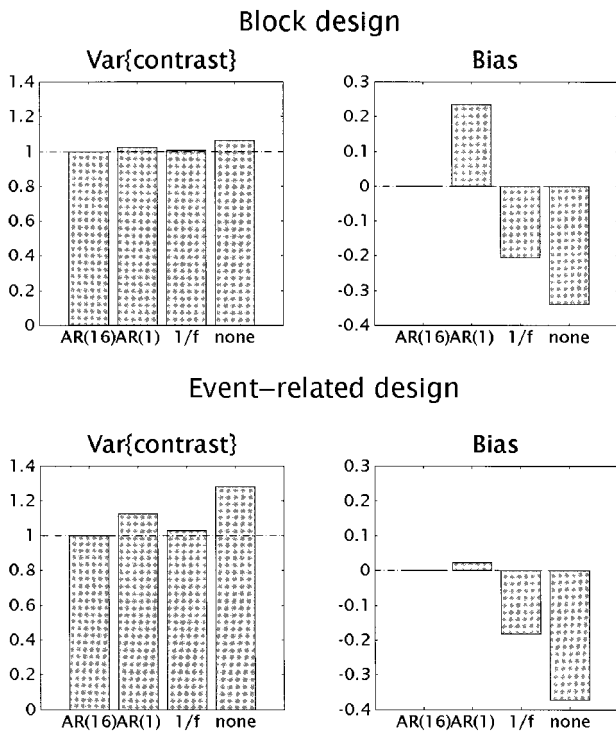


FIG. 4. Efficiencies and biases computed according to Eq. (3) and Eq. (4) in the main text for the regressors in Fig. 2 and contrasts of [1 0] and [0 1] for three models of intrinsic correlations [AR(16), AR(1), and the modified $1/f$ models] and assuming they do not exist (“none”). The results are for the Gauss–Markov estimators (i.e., using a whitening strategy based on the appropriate model in each case) using the first model [AR(16)] as an approximation to the true correlations. The contrast variances have been normalized to the minimum attainable. The bias and increased contrast variance induced result from adopting a whitening strategy when there is a discrepancy between the actual and the assumed intrinsic correlations.

and Friston, 1995). Generally if the regressors conform to these eigenvectors then there is no loss of efficiency.

The bias incurred by mis-specification can be substantial, resulting in an over- [AR(1)] or under- ($1/f$ and “none”) estimation of the contrast variance leading, in turn, to inexact tests using the associated T statistic that are unduly insensitive [AR(1)] or invalid ($1/f$ and “none”). The effect is not trivial. For example the bias engendered by assuming an AR(1) form in Fig. 4 is about 24%. This would result in about a 10% reduction of T values and could have profound effects on inference.

In summary the use of minimum variance, or maximum efficiency, filters can lead to invalid tests. This suggests that the use of whitening is inappropriate and the more important objective is to adopt filtering strategies that minimize bias to ensure that the tests are robust in the face of misspecified autocorrelation structures (i.e., their validity is retained). The minimum bias approach is even more tenable given that sensitivity in fMRI is not generally a great concern. This is

because a large number of scans enter into the estimation in fixed-effect analyses, and random-effects analyses (with fewer degrees of freedom) do not have to contend with serial correlations.

Minimum Bias Filters

There are two fundamental problems when trying to model intrinsic correlations: (i) one generally does not know the true intrinsic correlations and (ii) even if they were known for any given voxel time series, adopting the same assumptions for all voxels will lead to bias and loss of efficiency because each voxel has a different correlation structure (e.g., brain-stem voxels will be subject to pulsatile effects, ventricular voxels will be subject to CSF flow artifacts, white matter voxels will not be subject to neurogenic noise). It should be noted that very reasonable methods have been proposed for local estimates of spatially varying noise (e.g., Lange and Zeger, 1997). However, in this paper we assume that computational, and other, constraints require us to use the same statistical model for all voxels.

One solution to the “bias problem” is described in Worsley and Friston (1995) and involves conditioning the serial correlations by smoothing. This effectively imposes a structure on the intrinsic correlations that renders the difference between the assumed and the actual correlations less severe. Although generally less efficient, the ensuing inferences are less biased and therefore more robust. The loss of efficiency can be minimized by appropriate experimental design and choosing a suitable filter \mathbf{S} . In other words there are certain forms of temporal filtering for which $\mathbf{S}\mathbf{V}_i\mathbf{S}^T \approx \mathbf{S}\mathbf{V}_a\mathbf{S}^T$ even when \mathbf{V}_i is not known [see Eq. (4)]. These filters will minimize bias. The problem is to find a suitable form for \mathbf{S} .

One approach to designing a minimum bias filter is to treat the intrinsic correlation \mathbf{V}_i , not as an unknown deterministic variable, but as a random variable, whose distributional properties are known or can be estimated. We can then choose a filter that minimizes the expected square bias over all \mathbf{V}_i ,

$$\mathbf{S}_{\text{MB}} = \min \arg_{\mathbf{S}} \{ \xi\{\mathbf{S}\} \} \quad (5)$$

$$\xi\{\mathbf{S}\} = \int \text{bias}\{\mathbf{S}, \mathbf{V}_i\}^2 p(\mathbf{V}_i) d\mathbf{V}_i.$$

Equation (5) says that the ideal filter would minimize the expected or mean square bias over all intrinsic correlation structures encountered. An expression for mean square bias and the equivalent mean contrast variance (i.e., $1/\text{efficiency}$) is provided in Appendix C. This expression uses the first and second order moments of the intrinsic autocorrelation function, parameterized in terms of the underlying autoregression co-

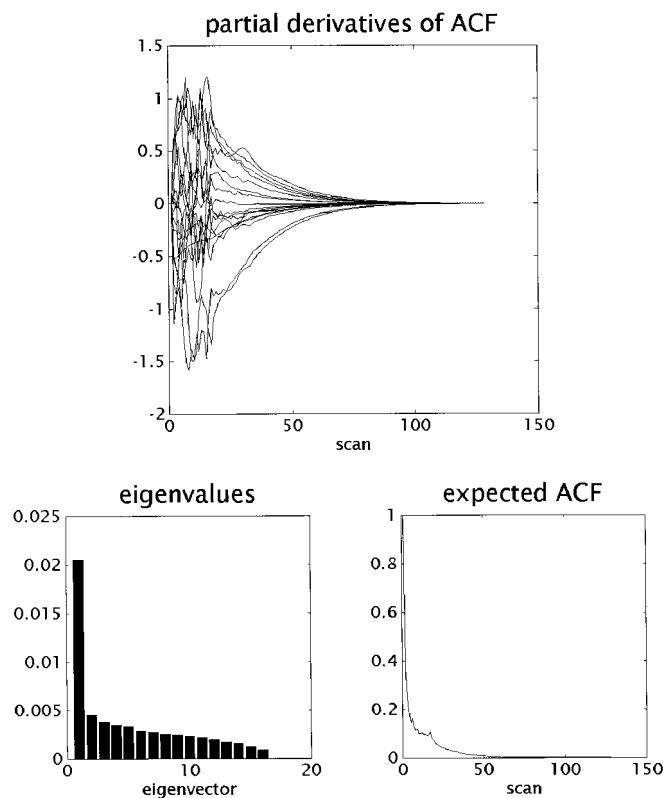


FIG. 5. Characterizing the variability in intrinsic correlations. Top: The 16 partial derivatives of the autocorrelation function with respect to the eigenvectors of the covariance matrix of the underlying autoregression coefficients. These represent changes to the autocorrelation function induced by the principal components of variation inherent in the coefficients. The covariances were evaluated over the voxels described in Fig. 2. Lower left: The associated eigenvalue spectrum. Lower right: The autocorrelation function associated with the mean of the autoregression coefficients. These characterizations enter into Eq. (C.3) in Appendix C, to estimate the mean square bias for a given filter.

efficients. More precisely, given the expected coefficients and their covariances, a simple second-order approximation to Eq. (5) obtains in terms of the eigenvectors and eigenvalues of the AR coefficient covariance matrix. These characterize the principal variations about the expected autocorrelation function. Empirical examples are shown in Fig. 5, based on the variation over gray matter voxels in the data used in Fig. 2. Here the principal variations, about the expected autocorrelation function (lower right), are presented (top) in terms of partial derivatives of the autocorrelation function with respect to the autoregressive eigenvectors (see Appendix C).

The expressions for mean square bias and mean contrast variance will be used in the next subsection to evaluate the behavior of three filtering schemes in relation to each other and a number of different correlation models. First however, we will use them to motivate the use of band-pass filtering: Intuitively one

might posit band-pass filtering as a minimum bias filter. In the limit of very narrow band-pass filtering the spectral densities of the assumed and actual correlations, after filtering, would be identical and bias would be negligible. Clearly this would be inefficient but suggests that some band-pass filter might be an appropriate choice. Although there is no single universal minimum bias filter, in the sense it will depend on the design matrix and contrasts employed and other data acquisition parameters; one indication of which frequencies can be usefully attenuated derives from examining how bias depends on the upper and lower cutoff frequencies of a band-pass filter.

Figure 6 shows the mean square bias and mean contrast variance incurred by varying the upper and lower band-pass frequencies. These results are based on the epoch-related regressors in Fig. 2 and assume that the intrinsic correlations conform to the AR(16) estimate. This means that any bias is due to variation

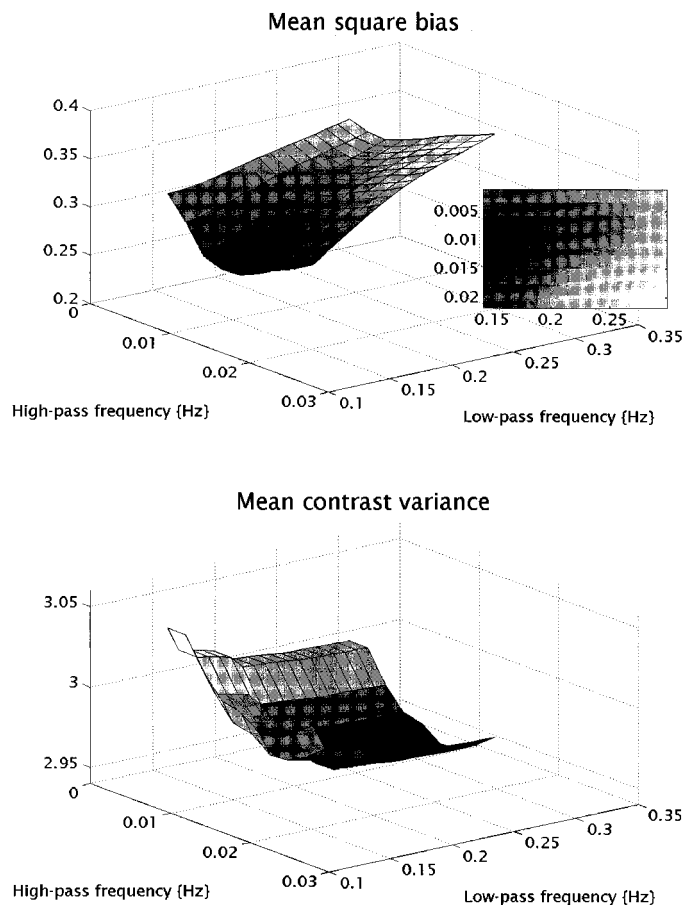


FIG. 6. Top: Mean square bias (shown in image format in inset) as a function of high- and low-pass cutoff frequencies defining a band-pass filter. Darker areas correspond to lower bias. Note that minimum bias attains when a substantial degree of smoothing or low-pass filtering is used in conjunction with high-pass filtering (dark area on the middle left). Bottom: As for the top but now depicting efficiency. The gray scale is arbitrary.

about that estimate and not due to specifying an inappropriately simple form for the correlations.³ The ranges of upper and lower band-pass frequencies were chosen to avoid encroaching on frequencies that contain signal. This ensured that efficiency was not severely compromised. The critical thing to note from Fig. 6 is that the effects of low-pass and high-pass filtering are not linearly separable. In other words low-pass filtering or smoothing engenders minimum bias but only in the context of high-pass filtering. It is apparent that the minimum bias obtains with the greatest degree of smoothing examined but only in conjunction with high-pass filtering, at around 1/96 per second. In short, band-pass filtering (as opposed to high- or low-pass filtering on their own) minimizes bias without a profound effect on efficiency. Interestingly, in this example, although increasing the degree of smoothing or low-pass filtering increases contrast variance (i.e., decreases efficiency), at high degrees of smoothing the minimum variance high-pass filter is very similar to the minimum bias filter (see Fig. 6).

These results used filter matrices that have a simple form in frequency space but are computationally expensive to implement. Next we describe a band-pass filter used in practice (e.g., in SPM99) and for the remainder of this paper.

Computationally Efficient Band-Pass Filters

The filter \mathbf{S} can be factorized into low- and high-pass⁴ components $\mathbf{S} = \mathbf{S}_L \mathbf{S}_H$. The motivation for this is partly practical and speaks to the special problems of fMRI data analysis and the massive amount of data that have to be filtered. The implementation of the filter can be made computationally much more efficient if the high frequencies are removed by a sparse Toeplitz convolution matrix and the high-pass component is implemented by regressing out low-frequency components. In this paper we choose \mathbf{S}_L so that its transfer function corresponds to that of the hemodynamic response function (the implied kernel is, however, symmetrical and does not induce a delay). This is a principled choice because it is in these frequencies that the neurogenic signal resides. \mathbf{S}_H is, effectively, the residual-forming matrix associated with a discrete cosine transform set (DCT) of regressors \mathbf{R} up to a frequency specified in term of a minimum period, expressed in seconds. In this paper we use a cutoff period

³ An AR(16) model stands in here for nearly every other possible model of intrinsic correlations. For example an AR(16) model can emulate the AR plus white noise model of Purdon and Weisskoff (1998).

⁴ The terms low- and high-pass filtering are technically imprecise because the linear filter matrices are not generally convolution matrices (i.e., \mathbf{S}_H does not have a Toeplitz form). However, they remove high- and low-frequency components, respectively.

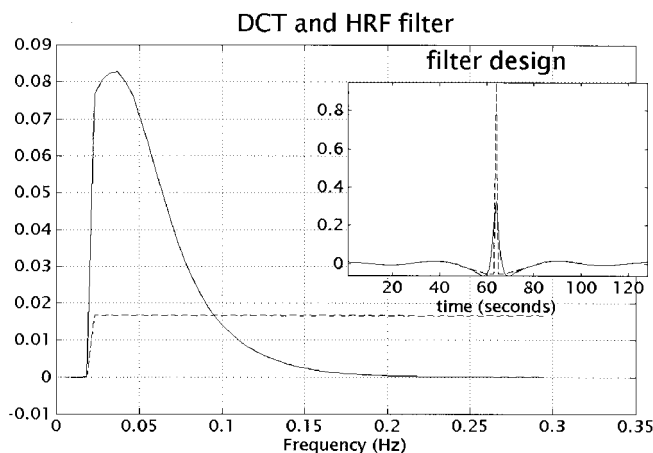


FIG. 7. The spectral density of a band-pass filter based on the hemodynamic response function in Fig. 1 (solid line) and a high-pass component with a cutoff at 1/64 Hz (broken line). The corresponding symmetrical filter kernels are shown in the inset for the high-pass filter (broken line) and band-pass filter (solid line).

of 64 s.⁵ Some people prefer the use of polynomial or spline models for drift removal because the DCT imposes a zero slope at the ends of the time series and this is not a plausible constraint. The (squared) transfer functions and kernels associated with the high-pass and combined high- and low-pass (i.e., band-pass) filters are shown in Fig. 7.

The effect of filtering the data is to impose an auto-correlation structure or frequency profile on the error terms. This reduces the discrepancy between the underlying serial correlations and those assumed by any particular model. This effect is illustrated in Fig. 8 in which the band-pass filter in Fig. 7 has been applied to the empirical time series used above. Filtering markedly reduces the differences among the spectral density and autocorrelation estimates using the various models (compare Fig. 8 with Fig. 3). The question addressed in the next subsection is whether this filter reduces mean square bias and, if so, at what cost in terms of mean efficiency.

An Evaluation of Different Filtering Strategies

In this subsection we examine the effect of filtering on mean contrast variance (i.e., mean 1/efficiency) and mean square bias using the expressions in Appendix C. This is effected under three different models of serial

⁵ In practice filtering is implemented as $\mathbf{S}\mathbf{y} \equiv \mathbf{S}_L \mathbf{S}_H \mathbf{y} \equiv \mathbf{S}_L (\mathbf{y} - \mathbf{R}(\mathbf{R}^T \mathbf{y}))$. This regression scheme eschews the need to actually form a large (nonsparse) residual-forming matrix associated with the DCT matrix \mathbf{R} . This form for \mathbf{S} can be implemented in a way that gives a broad range of frequency modulation for relatively small numbers of floating point operations. Note that \mathbf{R} is a unit orthogonal matrix. \mathbf{R} could comprise a Fourier basis set or indeed polynomials. We prefer a DCT set because of its high efficiency and its ability to remove monotonic trends.

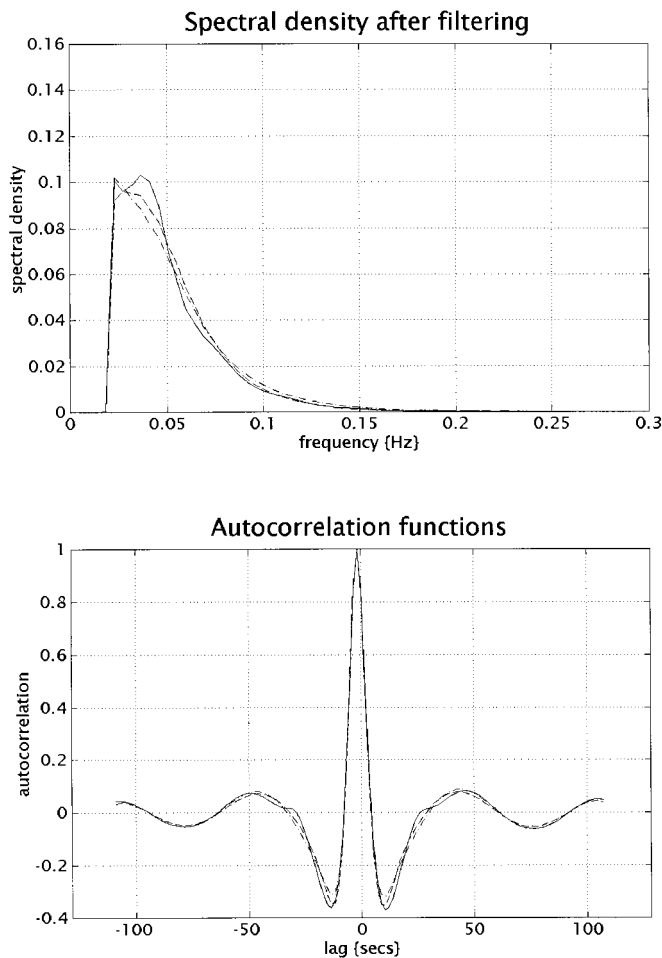


FIG. 8. The spectral density and autocorrelation functions predicted on the basis of the three models shown in Fig. 3, after filtering with the band-pass filter in Fig. 7. Compare these functions with those in Fig. 3. The differences are now ameliorated.

correlations: (i) AR(1), (ii) $1/f$, and (iii) AR(16). Again we will assume that the AR(16) estimates are a good approximation to the true intrinsic correlations. For each model we compared the effect of filtering the data with whitening. In order to demonstrate the interaction between high- and low-pass filtering we used a high-pass filter and a band-pass filter. The latter corresponds to high-pass filtering with smoothing. The addition of smoothing is the critical issue here: The high-pass component is motivated by considerations of both bias and efficiency. One might expect that high-pass filtering would decrease bias by removing low frequencies that are poorly modeled by simple models. Furthermore the effect on efficiency will be small because the minimum variance filter is itself a high-pass filter. On the other hand smoothing is likely to reduce efficiency markedly and its application has to be justified much more carefully.

The impact of filtering can be illustrated by parametrically varying the amount of filtering with a filter \mathbf{F} ,

where $\mathbf{S} = s \cdot \mathbf{F} + (1 - s)\mathbf{1}$; $\mathbf{1}$ is the identity matrix and s is varied between 0 (no filtering) and 1 (filtering with \mathbf{F}). The models and filters considered correspond to

$$\mathbf{V}_a = \begin{cases} \mathbf{V}_{\text{AR}(1)} \\ \mathbf{V}_{1/f} \\ \mathbf{V}_{\text{AR}(16)} \end{cases} \quad \text{and} \quad \mathbf{F} = \begin{cases} \mathbf{V}_a^{-1/2} & \text{“whitening”} \\ \mathbf{S}_H & \text{“high-pass”} \\ \mathbf{S}_L \mathbf{S}_H & \text{“band-pass”} \end{cases}.$$

Mean square bias and mean contrast variance are shown as functions of the filtering parameter s in Fig. 9 for the various schema above. The effect on efficiency is remarkably consistent over the models assumed for the intrinsic correlations. The most efficient filter is a whitening filter that progressively decreases the expected contrast variance. High-pass filtering does not

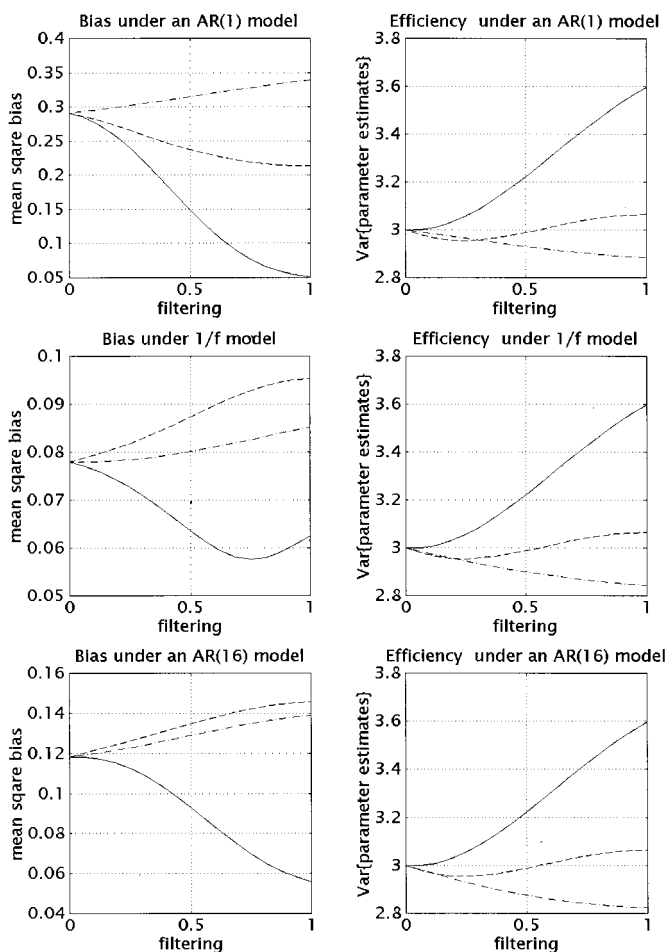


FIG. 9. The effect of filtering on mean square bias and mean contrast variance when applying three filters: the band-pass filter in Fig. 8 (solid lines), the high-pass filter in Fig. 8 (dashed lines), and a whitening filter appropriate to the model assumed for the intrinsic correlations (dot-dash lines). Each of these filters was applied under three models: an AR(1) model (top), a modified $1/f$ model (middle), and an AR(16) model (bottom). The expected square biases (left) and contrast variances (right) were computed as described in Appendix C and plotted against a parameter s that determines the degree of filtering applied (see main text).

markedly change this mean contrast variance and renders the estimation only slightly less efficient than no filtering at all. The addition of smoothing to give band-pass filtering decreases efficiency by increasing the mean contrast variance by about 15%. The effects on mean square bias are similarly consistent. Whitening attenuates mean square bias slightly. High-pass filtering is more effective at attenuating bias but only for the AR(1) model. This is because the whitening filters for the $1/f$ and AR(16) models more closely approximate the high-pass filter. The addition of smoothing engenders a substantial and consistent reduction in bias, suggesting that, at least for the acquisition parameters implicit in these data, smoothing has an important role in minimizing bias. This is at the expense of reduced efficiency.

The profiles at the bottom in Fig. 9 are interesting because, as in the analysis presented in Fig. 6, the mean intrinsic correlations and assumed autocorrelation structure are taken to be the same. This means that any effects on bias or efficiency are due solely to variations about that mean (i.e., the second term in Eq. (C.3), Appendix C). The implication is that even a sophisticated autocorrelation model will benefit, in terms of inferential bias, from the particular band-pass filtering considered here.

Spatially Varying Intrinsic Correlations

In the illustrative examples above we have assumed that the variation within one voxel, over realizations, can be approximated by the variation over realizations in different gray-matter voxels that show a degree of functional homogeneity. The second problem, introduced at the beginning of this section, is that even if we assume the correct form for one voxel then we will be necessarily incorrect for every other voxel in the brain. This reflects the spatially dependent nature of temporal autocorrelations (see also Locascio *et al.*, 1997). Assuming the same form for all voxels is a special constraint under which analyses of fMRI data have to operate. This is because we would like to use the same statistical model for every voxel. There are both computational and theoretical reasons for this, which derive from the later use of Gaussian Field theory when making inferences that are corrected for the volume analyzed. The theoretical reasons are that different intrinsic correlations would lead to statistics with different (effective) degrees of freedom at each voxel. Whether Gaussian Field theory is robust to this effect remains to be addressed.

Not only does appropriate temporal filtering reduce bias engendered by misspecification of the intrinsic correlations at any one voxel, and stochastic variations about that specification, but it also addresses the problem of spatially varying serial correlations over voxels.

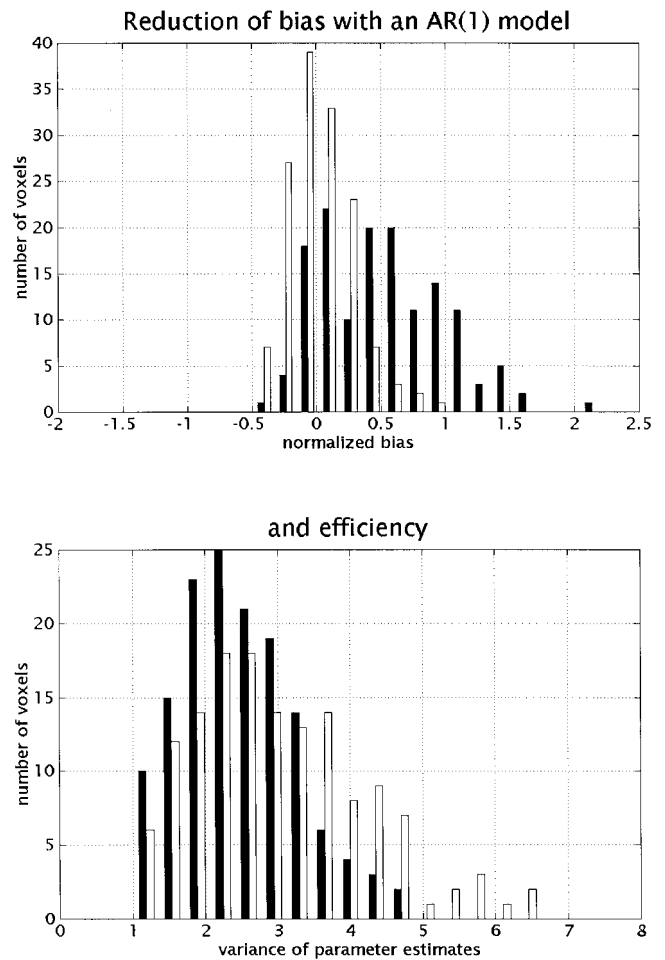


FIG. 10. The distribution of bias (top) and contrast variance (bottom) over voxels using an AR(16) model to estimate intrinsic correlations at 512 voxels and assuming the same AR(1) autocorrelation structure over voxels. Distributions are shown with band-pass filtering (open bars) and with whitening (filled bars). Note how band-pass filtering reduces bias (at the expense of reduced efficiency). Efficiency is proportional to the inverse of the contrast variance.

The top of Fig. 10 shows bias, computed using Eq. (3) over 512 voxels using an AR(16) voxel-specific estimate for the intrinsic correlations \mathbf{V}_i and an AR(1) model averaged over all voxels for the assumed correlations \mathbf{V}_a . With whitening the biases (solid bars) range from -50 to 250% . With band-pass filtering (open bars) they are reduced substantially. The effect on efficiency is shown at the bottom. Here filtering increases the contrast variance in a nontrivial way (by as much as 50% in some voxels). It is interesting to note that spatially dependent temporal autocorrelations render the efficiency very variable over voxels (by nearly an order of magnitude). This is important because it means that fMRI is not homogeneous in its sensitivity to evoked responses from voxel to voxel, simply because of differences in serial correlations.

DISCUSSION

This paper has addressed temporal filtering in fMRI time-series analysis. Whitening serially correlated data is the most efficient approach to parameter estimation. However, whitening can render the analysis sensitive to inferential bias, if there is a discrepancy between the assumed and the actual autocorrelations. This bias, although not expressed in terms of the estimated model parameters, has profound effects on any statistic used for inference. The special constraints of fMRI analysis ensure that there will always be a misspecification of the intrinsic autocorrelations because of their spatially varying nature over voxels. One resolution of this problem is to filter the data to ensure bias is small while maintaining a reasonable degree of efficiency.

Filtering can be chosen in a principled way to maintain efficiency while minimizing bias. Efficiency can be retained by band-pass filtering to preserve frequency components that correspond to signal (i.e., the frequencies of the HRF) while suppressing high- and low-frequency components. By estimating the mean square bias over the range of intrinsic autocorrelation functions that are likely to be encountered, it can be shown that supplementing a high-pass filter with smoothing has an important role in reducing bias.

The various strategies that can be adopted can be summarized in terms of two choices: (i) the assumed form for the intrinsic correlations \mathbf{V}_a and (ii) the filter applied to the data \mathbf{S} . Permutations include

$$\mathbf{V}_a = \begin{cases} \mathbf{1} \\ \mathbf{1} \\ \mathbf{V}_{\text{AR}(p)} \\ \mathbf{V}_{\text{AR}(p)} \end{cases},$$

$$\mathbf{S} = \begin{cases} \mathbf{1} & \text{ordinary least squares} \\ \mathbf{S}_L \mathbf{S}_H & \text{conventional "filtering" (SPM97)} \\ \mathbf{K}_{\text{AR}(p)}^{-1} & \text{conventional "whitening"} \\ \mathbf{S}_L \mathbf{S}_H & \text{band-pass filtering (SPM99)} \end{cases},$$

where the assumed form is an AR(p) model. The last strategy, adopted in SPM99, is motivated by a balance between efficiency and computational expediency. Because the assumed correlations \mathbf{V}_a do not enter explicitly into the computation of the parameter estimates but only into the subsequent estimation of their standard error (and ensuing T or F statistics), the autocorrelation structure and parameter estimation can be implemented in a single pass through the data. SPM99 has the facility to use an AR(1) estimate of intrinsic correlations, in conjunction with (separately) specified high- and low-pass filtering.

A further motivation for filtering the data, to exert some control over the variance–bias trade-off, is that the exact form of serial correlations will vary with

scanner, acquisition parameters, and experiment. For example the relative contribution of aliased bio-rhythms will change with TR and field strength. By explicitly acknowledging a discrepancy between the assumed approximation to underlying correlations a consistent approach to data analysis can be adopted over a range of experimental parameters and acquisition systems.

The issues considered in this paper apply even when the repetition time (TR) or interscan interval is long. This is because serial correlations can enter as low-frequency components, which are characteristic of all fMRI time series, irrespective of the TR. Clearly as the TR gets longer, higher frequencies cease to be a consideration and the role of low-pass filtering or smoothing in reducing bias will be less relevant.

The conclusions presented in this paper arise under the special constraints of estimating serial correlations in a linear framework and, more specifically, using estimators that can be applied to all voxels. The inherent trade-off between the efficiency of parameter estimation and bias in variance estimation is shaped by these constraints. Other approaches using, for example, nonlinear observation models, may provide more efficient and unbiased estimators than those we have considered.

It should be noted that the main aim of this paper is to provide an analytical framework within which the effects of various filtering strategies on bias and efficiency can be evaluated. We have demonstrated the use of this framework using only one data set and do not anticipate that all the conclusions will necessarily generalize to other acquisition parameters or statistical models. What has been shown here is, however, sufficient to assert that, for short repetition times, band-pass filtering can have an important role in ameliorating inferential bias and consequently in ensuring the relative robustness of the resulting statistical tests.

APPENDIX A

Forms of Intrinsic and Assumed Autocorrelations

A distinction is made between the true intrinsic autocorrelations in a fMRI time series of length n and those assumed. These correlations are characterized by the $(n \times n)$ convolution matrices \mathbf{K}_i and \mathbf{K}_a , respectively, with an ensuing noise process $\epsilon = \mathbf{K}_i \mathbf{z}$, where \mathbf{z} , is an independent innovation $\sim \mathcal{N}(0, \sigma^2 \mathbf{I})$ and $\text{diag}\{\mathbf{K}_i \mathbf{K}_i^T\} = \mathbf{1}$. The corresponding autocorrelation matrices are $\mathbf{V}_i = \mathbf{K}_i \mathbf{K}_i^T$ and $\mathbf{V}_a = \mathbf{K}_a \mathbf{K}_a^T$. In this appendix we describe some models of intrinsic autocorrelations, specifically p th order autoregressive models AR(p) [e.g., AR(1); Bullmore *et al.*, 1996] or those that derive from characterizations of noise autocovariance structures or equivalently their spectral density (Zarahn *et al.*, 1997). For any process the spectral density $g(\omega)$ and

autocorrelation function $\rho(t)$ are related by the Fourier transform pair

$$\rho(t) = FT\{g(\omega)\}, \quad g(\omega) = IFT\{\rho(t)\}, \quad (\text{A.1})$$

where $\mathbf{V} = \text{Toeplitz}\{\rho(t)\}$ and $\mathbf{K} = \mathbf{V}^{1/2}$.

Here $t = [0, 1, \dots, n-1]$ is the lag in scans with $\rho(0) = 1$ and $\omega = 2\pi i$ ($i = [0, \dots, n-1]$) denotes frequency. The *Toeplitz* operator returns a Toeplitz matrix (i.e., a matrix that is symmetrical about the leading diagonal). The transfer function associated with the linear filter \mathbf{K} is $l(\omega)$, where $g(\omega) = |l(\omega)|^2$.

Autoregressive Models

Autoregressive models have the following form:

$$\epsilon = \mathbf{A}\epsilon + \mathbf{z} \Leftrightarrow \epsilon = (\mathbf{I} - \mathbf{A})^{-1}\mathbf{z},$$

giving $\mathbf{K}_a \propto (\mathbf{I} - \mathbf{A})^{-1}$ where \mathbf{A}

$$= \begin{bmatrix} 0 & 0 & 0 & 0 & \dots \\ a_1 & 0 & 0 & 0 & \\ a_2 & a_1 & 0 & 0 & \\ a_3 & a_2 & a_1 & 0 & \\ \vdots & & & & \ddots \end{bmatrix}. \quad (\text{A.2})$$

The autoregression coefficients in the triangular matrix \mathbf{A} can be estimated using

$$\mathbf{a} = [a_1, \dots, a_p]$$

$$= \begin{bmatrix} 1 & \rho(1) & \dots & \rho(p) \\ \rho(1) & 1 & & \vdots \\ \vdots & & \ddots & \rho(1) \\ \rho(p) & \dots & \rho(1) & 1 \end{bmatrix}^{-1} \begin{bmatrix} \rho(1) \\ \rho(2) \\ \vdots \\ \rho(p+1) \end{bmatrix}. \quad (\text{A.3})$$

The corresponding spectral density over n frequencies is given by

$$g(\omega) = |FT_n\{[1, -\mathbf{a}]\}|^{-2}, \quad (\text{A.4})$$

where $FT_n\{\cdot\}$ is a n -point Fourier transform with zero padding (cf. the Yule–Walker method of spectral density estimation). With these relationships [(A.1) to (A.3)] one can take any empirical estimate of the autocorrelation function $\rho(t)$ and estimate the autoregression model-specific convolution \mathbf{K}_a and autocorrelation $\mathbf{V}_a = \mathbf{K}_a \mathbf{K}_a^T$ matrices.

Modified 1/f Models

\mathbf{K}_a and \mathbf{V}_a can obviously be estimated using spectral density through Eq. (A.1) if the model of autocorrelations is expressed in frequency space; here we use the analytic form suggested by the work of Zarahn *et al.* (1997),

$$|s(\omega)| = \frac{q_1}{\omega} + q_2, \quad \text{where } g(\omega) = |s(\omega)|^2. \quad (\text{A.5})$$

Note that Eq. (A.5) is linear in the parameters which can therefore be estimated in an unbiased manner using ordinary least squares.

APPENDIX B

Efficiency and Bias

In this section we provide expressions for the efficiency and bias for any design matrix \mathbf{X} and any contrast of parameter estimates specified with a vector of contrast weights \mathbf{c} (this framework serves all the filtering schemes outlined in the main text). These expressions are developed in the context of the general linear model and parametric statistical inference (Friston *et al.*, 1995). The bias here is in terms of the estimated standard error associated with any ensuing statistic. Consider the general linear model,

$$\mathbf{S}\mathbf{y} = \mathbf{S}\mathbf{X}\beta + \mathbf{S}\mathbf{K}_i\mathbf{z}, \quad (\text{B.1})$$

where \mathbf{y} is the response variable and \mathbf{S} is an applied filter matrix. The efficiency of the general least squares contrast estimator $\mathbf{c}^T \hat{\beta}_{\text{GLS}}$ is inversely proportional to its variance,

$$\text{Efficiency} \propto \text{Var}\{\mathbf{c}^T \hat{\beta}_{\text{GLS}}\}^{-1}$$

$$\text{Var}\{\mathbf{c}^T \hat{\beta}_{\text{GLS}}\} = \sigma^2 \mathbf{c}^T (\mathbf{S}\mathbf{X})^+ \mathbf{S}\mathbf{V}_i \mathbf{S}^T (\mathbf{S}\mathbf{X})^+ \mathbf{c}, \quad (\text{B.2})$$

where $^+$ denotes the pseudoinverse. Efficiency is maximized with the Gauss–Markov estimator, when $\mathbf{S} = \mathbf{K}_i^{-1}$ if the latter were known. However, there is another important consideration: The variance of the contrast has to be estimated in order to provide for statistical inference. This estimator and its expectation are

$$\hat{\text{Var}}\{\mathbf{c}^T \hat{\beta}\}$$

$$= \frac{\mathbf{y}^T \mathbf{S}^T \mathbf{R}^T \mathbf{R} \mathbf{S} \mathbf{y}}{\text{trace}\{\mathbf{R} \mathbf{S} \mathbf{V}_a \mathbf{S}^T\}} \mathbf{c}^T (\mathbf{S}\mathbf{X})^+ \mathbf{S}\mathbf{V}_a \mathbf{S}^T (\mathbf{S}\mathbf{X})^+ \mathbf{c}$$

$$\langle \hat{\text{Var}}\{\mathbf{c}^T \hat{\beta}\} \rangle$$

$$= \frac{\sigma^2 \text{trace}\{\mathbf{R} \mathbf{S} \mathbf{V}_i \mathbf{S}^T\}}{\text{trace}\{\mathbf{R} \mathbf{S} \mathbf{V}_a \mathbf{S}^T\}} \mathbf{c}^T (\mathbf{S}\mathbf{X})^+ \mathbf{S}\mathbf{V}_a \mathbf{S}^T (\mathbf{S}\mathbf{X})^+ \mathbf{c}, \quad (\text{B.3})$$

where $\mathbf{R} = \mathbf{I} - \mathbf{S}\mathbf{X}(\mathbf{S}\mathbf{X})^+$ is a residual-forming matrix. Bias can be expressed in terms of the (normalized) difference between the actual and the expected contrast variance estimators,

$Bias\{\mathbf{S}, \mathbf{V}_i\}$

$$= \frac{Var\{\mathbf{c}^T \hat{\beta}_{GLS}\} - \langle \hat{Var}\{\mathbf{c}^T \hat{\beta}_{GLS}\} \rangle}{Var\{\mathbf{c}^T \hat{\beta}_{GLS}\}} \quad (\text{B.4})$$

$$= 1 - \frac{trace\{\mathbf{R}\mathbf{S}\mathbf{V}_i\mathbf{S}^T\}\mathbf{c}^T(\mathbf{S}\mathbf{X}) + \mathbf{S}\mathbf{V}_i\mathbf{S}^T(\mathbf{S}\mathbf{X}) + T\mathbf{c}}{trace\{\mathbf{R}\mathbf{S}\mathbf{V}_i\mathbf{S}^T\}\mathbf{c}^T(\mathbf{S}\mathbf{X}) + \mathbf{S}\mathbf{V}_i\mathbf{S}^T(\mathbf{S}\mathbf{X}) + T\mathbf{c}}.$$

The critical thing about Eq. (B.4) is that bias is reduced as \mathbf{S} induces more correlations relative to \mathbf{V}_i . In other words there are certain forms of temporal filtering for which $\mathbf{S}\mathbf{V}_i\mathbf{S}^T \approx \mathbf{S}\mathbf{V}_a\mathbf{S}^T$ even if $\mathbf{V}_i \neq \mathbf{V}_a$. In extreme cases this allows one to essentially ignore intrinsic correlations with temporal filtering (i.e., $\mathbf{V}_a = \mathbf{I}$) although this strategy may be inefficient. Generally bias becomes sensitive to discrepancies between the actual and the assumed correlations when no filtering is employed and exquisitely so when \mathbf{S} is a deconvolution matrix (e.g., whitening under the wrong assumptions about \mathbf{V}_i).

APPENDIX C

Mean Square Bias

In Appendix B the expression for bias treated \mathbf{V}_i as a fixed deterministic variable. In this appendix we derive an approximation for the expected squared bias when \mathbf{V}_i is a random stochastic variable parameterized in terms of its AR coefficients \mathbf{a} . Let

$$f(\mathbf{r}, \mathbf{S}) = Bias\{V\{\bar{\mathbf{a}} + \mathbf{Q}\mathbf{r}\}, \mathbf{S}\}^2. \quad (\text{C.1})$$

The operator $V\{\mathbf{a}\}$ returns the autocorrelation matrix given the underlying AR coefficients according to A.2. $\bar{\mathbf{a}}$ are the expected coefficients and \mathbf{Q} contains the eigenvectors of $Cov\{\mathbf{a}\} = \langle (\mathbf{a} - \bar{\mathbf{a}}) \cdot (\mathbf{a} - \bar{\mathbf{a}})^T \rangle$ such that

$$\mathbf{r} = \mathbf{Q}^T(\mathbf{a} - \bar{\mathbf{a}}) \Rightarrow \begin{cases} \langle \mathbf{r} \rangle = \mathbf{0} \\ \langle \mathbf{r} \cdot \mathbf{r}^T \rangle = \lambda \end{cases} \quad (\text{C.2})$$

and λ is a leading diagonal matrix of associated eigenvalues. Mean square bias is approximated with

$$\xi(\mathbf{S}) = \langle f(\mathbf{r}, \mathbf{S}) \rangle_r \approx f(\mathbf{0}, \mathbf{S}) + \sum_i \frac{\lambda_i}{2} \frac{\partial^2 f(\mathbf{0}, \mathbf{S})}{\partial r_i^2}. \quad (\text{C.3})$$

This follows from taking the expectation of the second-order approximation of the Taylor expansion of Eq. (C.1) around $\mathbf{r} = \mathbf{0}$ and substituting the expectations in Eq. (C.2). Note that, apart from the second-order approximation, no distributional assumptions have been made about the intrinsic AR coefficients. If these coefficients had a multivariate Gaussian distribution then (C.3) would be exactly right. The first term in (C.3) reflects the mean square bias attributable to the deviation between

the assumed and the expected autocorrelation function. The second term reflects the contribution to bias due to variation about that expectation. An equivalent expression for mean contrast estimate variance obtains by substituting Eq. (B.2) into Eq. (C.1).

In this paper the expectation and covariances of the AR coefficients were determined empirically using multiple realizations over gray-matter voxels and an AR(16) model. The partial derivatives in C.3 were estimated numerically.

ACKNOWLEDGMENTS

K.J.F., O.J., and A.P.H., were funded by the Wellcome trust. We thank the two anonymous reviewers for guidance in the development and presentation of this work.

REFERENCES

- Aguirre, G. K., Zarahn, E., and D'Esposito, M. 1997. Empirical analysis of BOLD fMRI statistics. II. Spatially smoothed data collected under the null hypothesis and experimental conditions. *NeuroImage* **5**: 199–212.
- Boynton, G. M., Engel, S. A., Glover, G. H., and Heeger, D. J. 1996. Linear systems analysis of functional magnetic resonance imaging in human V1. *J. Neurosci.* **16**: 4207–4221.
- Bullmore, E. T., Brammer, M. J., Williams, S. C. R., Rabe-Hesketh, S., Janot, N., David, A., Mellers, J., Howard, R., and Sham, P. 1996. Statistical methods of estimation and inference for functional MR images. *Magn. Reson. Med.* **35**: 261–277.
- Friston, K. J., Jezzard, P. J., and Turner, R. 1994. Analysis of functional MRI time-series. *Hum. Brain Mapp.* **1**: 153–171.
- Friston, K. J., Holmes, A. P., Worsley, K. J., Poline, J. B., Frith, C. D., and Frackowiak, R. S. J. 1995. Statistical parametric maps in functional imaging: A general linear approach. *Hum. Brain Mapp.* **2**: 189–210.
- Friston, K. J., Josephs, O., Rees, G., and Turner, R. 1998. Non-linear event-related responses in fMRI. *Magn. Reson. Med.* **39**: 41–52.
- Holmes, A. P., Josephs, O., Büchel, C., and Friston, K. J. 1997. Statistical modelling of low frequency confounds in fMRI. *NeuroImage* **5**: S480.
- Josephs, O., Turner, R., and Friston, K. J. 1997. Event-related fMRI. *Hum. Brain Mapp.* **5**: 243–248.
- Lange, N., and Zeger, S. 1997. Non-linear Fourier time series analysis for human brain mapping with functional MRI. *Appl. Stats.* **46**: 1–26.
- Lawson, C. L., and Hanson, R. J. 1974. *Solving Least Squares Problems*. Prentice Hall, New York.
- Locascio, J. J., Peggy, J., and Corkin, S. 1997. A method of adjusting for temporal and spatial correlations in analysis of mean fMRI signal intensity changes. *NeuroImage* **3**: S76.
- Paradis, A.-L., Van de Morrtele, P.-F., Le Bihan, D., and Poline, J.-B. 1998. Do high temporal frequencies of the event-related fMRI response have a more specific spatial localization. *NeuroImage* **7**: S606.
- Purdon, P. L., and Weisskoff, R. 1998. Effect of temporal autocorrelations due to physiological noise stimulus paradigm on voxel-level false positive rates in fMRI. *Hum. Brain Mapp.* **6**: 239–249.
- Worsley, K. J., and Friston, K. J. 1995. Analysis of fMRI time-series revisited—Again. *NeuroImage* **2**: 173–181.
- Zarahn, E., Aguirre, G. K., and D'Esposito, M. 1997. Empirical analyses of BOLD fMRI statistics. I. Spatially unsmoothed data collected under null-hypothesis conditions. *NeuroImage* **5**: 179–197.